DOE/ER/54108--T1

DOE/ER/54108--T1

DE92 007280

Final Report to OFE, DOE: Effects of energetical particles on ballooning modes in high temperature tokamaks

Contract Number: DE-FG03-90ER~~54018~~ 54108

SAIC Project No. 01-0624-08-0302

Period of Performance: August 1990 to August 1991

K. T. Tsang
Applied Physics Operation
Science Applications International Corporation
1710 Goodridge Drive, McLean, VA 22102

January 22, 1992

EXECUTIVE SUMMARY

This report describes the work done by Science Applications International Corporation to study the effects of energetic particles on the microstability of a high temperature tokamak.

The effects of an energetic particle population on ballooning modes in a large aspect ratio, shifted circular flux surface tokamak equilibrium are investigated with the newly developed gyrokinetic numerical technique. The gyrokinetic equations for the background ion and electron, as well as that of the energetic population are solved directly as an initial value problem. The energetic particles are modeled with a slowdown distribution in energy. It is found that the ballooning mode stability of the plasma with an energetic species of increasing concentration does not differ much from an increase in the background plasma beta, except for possible energetic particle drift resonances. This result is encouraging to the idea that energetic particles such as alphas may be used to stabilize the ballooning modes in a fusion reactor.

I. INTRODUCTION

This report describes the work done by Science Applications International Corporation to study the effects of energetic particles on the microstability of a high temperature tokamak during the period from August 1990 to August 1991.

In recent high temperature tokamak experimental devices or future reactors, a population of energetic particles produced either as fusion byproducts or from neutral beam injection is significant enough to influence the equilibrium and stability substantially. These energetic particles are initially born with energies much in excess of that of the background plasma. As they are slowed down by collisions with the background plasma, most of their energy can be converted into plasma thermal energy. However, the free energy associated with this slowed-down energetic particle distribution may serve to destabilize the magnetohydrodynamic (MHD) ballooning modes or other drift modes, leading to anomalous loss of the energetic particles and/or the deterioration of background plasma confinement.

The effects of alpha or energetic particles on the stability of MHD ballooning modes in high temperature tokamak plasmas were first studied by Tsang and Sigmar[1] with a model that included only the perturbed electrostatic potential and parallel component of the magnetic vector potential. It was found that energetic particles could have a strong stabilizing effect on the MHD ballooning modes. Later study by Conner et al.[2] supported a similar conclusion with a similar model. Rosenbluth et al.[3] included the compressibility of the energetic particles and suggested that the energetic species can stabilize the ballooning modes just as the hot electron ring provides stability for the toroidal core plasma in the ELMO bumpy torus[4]. These earlier favorable results were contrasted with more recent and pessimistic results of Spong et al.[5], who expanded the work of Rosenbluth et al.[3] to include the energetic ions magnetic drift resonance in the ballooning mode equation. They found that in the limit, when the averaged energetic particle energy is much higher than that of the background ions, the stabilizing influence of the energetic particles on the ballooning modes was recovered. However, for temperature ratio between the energetic component and the core plasma exceeding 100 and moderate values of the energetic pressure, Spong et al. found that the alpha magnetic drift resonance can destabilize the MHD ballooning modes, leading to lower critical beta and closing the path to the second stability regime. This pessimistic prediction of lower critical beta by the effects of alpha particles on the MHD ballooning modes was confirmed by recent work of Rewoldt[6].

The calculations described in the previous paragraph are all based on an approximated solution of the perturbed energetic ion distribution function using expansion technique. In particular, the energetic bounce (or transit) frequency is assumed to be much higher than all other frequencies involved. This is not true for the magnetic drift frequency of the energetic particles because of the high energy these particles possess. In this work, we shall investigate the stability by taking advantage of the recent successful development of numerical gyrokinetic technique [7] that allows us to solve for the distribution functions without approximation

in the time domain as an initial value problem. In contrast to the traditional eigenmode stability study, any unstable mode will gradually appear and establish itself starting from the initial noise level using the gyrokinetic approach, just as in the particle-simulation approach. Using proper diagnostic techniques, we can distinguish different modes by their characteristics such as parity and mode frequency. In this way low frequency drift and ballooning stability of the energetic-core plasma system can be carefully studied.

II. GYROKINETIC MODEL

For low frequency electromagnetic stability in an axisymmetric large-aspect-ratio tokamak, $\epsilon = r/R \ll 1$, we use a toroidal (r, θ, ζ) coordinate system, where r is the minor radius, θ the poloidal angle, and ζ the toroidal angle. The magnetic surfaces are circles of radius r but with centers displaced by $\Delta(r)$. The poloidal angle θ is introduced so that $R = R_0 + rcos\theta + \Delta$, where R_0 is the major radius of the magnetic axis ($r = 0$) and R is the local major radius at (r, θ). The equilibrium toroidal magnetic field is given by $\vec{B}_t = B_0(1 - \epsilon cos\theta)\hat{\zeta}$, and the poloidal field is $B_p = B_\theta(r)[1 - (\Delta' + \epsilon)cos\theta]$, where $\Delta' \sim \epsilon$, but $r\Delta'' \sim 1$. To lowest order in ϵ the safety factor is $q = \epsilon B_0/B_\theta$.

Since most microinstabilities in tokamak plasmas have very short wavelengths perpendicular to the sheared magnetic field $\vec{B}$ compared with the parallel wavelengths ($k_\parallel/k_\perp << 1$, where $k_\parallel$ and $k_\perp$ are the parallel and perpendicular wavenumbers respectively), periodicity in the θ and ζ directions cannot be satisfied simultaneously. This difficulty is resolved by the so-called ballooning representation[8] in which any perturbed quantity, ϕ, is first Fourier decomposed in the ignorable coordinate, ζ, then the θ dependence is represented as an infinite sum of nonperiodic functions that add up to a periodic function, i. e.,

$$\phi(\theta, \zeta) = \sum_{p=-\infty}^{+\infty} \hat{\phi}(\theta - 2\pi p) exp(il\zeta), \tag{1}$$

where $\hat{\phi}$ is a function of an extended θ, which varies from -∞ to +∞, and l is the toiroidal mode number. To ensure convergence of this sum, $\hat{\phi}$ must vanish sufficiently fast as $\theta \rightarrow \pm\infty$. This representation is valid for high mode number perturbations in tokamaks and has the advantage that the usual poloidal mode coupling in the tokamak geometry is incorporated naturally.

Under the ballooning representation, the ion gyrokinetic equation[9] can be written as:

$$\frac{\partial h_i}{\partial t} = -\frac{v_\parallel}{Rq}\frac{\partial}{\partial\theta}(h_i + \frac{e}{T_i}\Phi_i F_i) - i\omega_{di}h_i + i(\omega_{*i}^T - \omega_{di})\frac{e}{T_i}\Phi_i F_i, \tag{2}$$

where

$$\Phi_i = (\phi - \frac{v_\parallel}{c}A_\parallel)J_{0i} + \frac{v_\perp}{k_\perp c}B_\parallel J_{1i}, \tag{3}$$

h_i is the nonadiabatic part of the perturbed ion distribution, f_i, defined by

$$f_i = -\frac{e\phi}{T_i}F_i + (h_i + \frac{c}{T_i}\Phi_i F_i)J_{0i}, \tag{4}$$

and the equilibrium distribution function is assumed to be a local Maxwellian :

$$F_i(v^2, r) = N_i(r)[M_i/2\pi T_i(r)]^{3/2} exp[-M_i v^2/2T_i(r)].$$

In the equations above, ϕ is the perturbed electrostatic potential, $B_\parallel$ is the perturbed parallel magnetic field, $A_\parallel$ is the perturbed parallel vector potential, T_i is the ion temperature, $k_\perp = k_\theta[1 + g_\theta^2]^{1/2}$ is the perpendicular wavenumber, $k_\theta = lq/r, \omega_{di} = lq(v_\parallel^2 + v_\perp^2)(cos\theta + g_\theta sin\theta)/rR\Omega$ is the ion magnetic drift frequency, $\omega_{*i}^T = \omega_{*i}[1 + \eta_i(M_i v^2/2T_i - 3/2)], \omega_{*i} = (lqcT_i/reB)\partial lnN_i/\partial r$ is the ion diamagnetic drift frequency, $\eta_i = \partial lnT_i/\partial lnN_i$ is the ion temperature gradient parameter, J_{0i} and J_{1i} are the Bessel functions with the argument $k_\perp v_\perp/\Omega$, $\Omega = eB/M_i c$, c is the speed of light, e is the magnitude of the electronic charge, $s = rq'/q$ is the shear parameter, $g_\theta = s\theta + \alpha sin\theta$ and $\alpha = -2Rq^2P'/B^2$, where P' is the gradient of the total pressure normal to the flux surface. The underlying equilibrium model being used here is that of a shifted circular flux surface that consistently reflects the changes in the equilibrium parameters as the plasma beta varies and has been used extensively in ballooning mode stability studies[10,11].

For the electrons, the gyrokinetic equation takes a simpler form, known as the drift kinetic equation, because the finite electron radius effects can be ignored:

$$\frac{\partial h_e}{\partial t} = -\frac{v_\parallel}{Rq}\frac{\partial}{\partial\theta}(h_i - \frac{e}{T_e}\Phi_e F_e) - i\omega_{de}h_e - i(\omega_{*e}^T - \omega_{de})\frac{e}{T_e}\Phi_e F_e, \tag{5}$$

where

$$\Phi_e = \phi - \frac{v_\parallel}{c}A_\parallel + (\frac{v_\perp}{v_e})^2\frac{B_\parallel}{B}\frac{T_e}{e}, \tag{6}$$

and h_e is the nonadiabatic part of the perturbed ion distribution f_e defined by

$$f_e = h_e + (\frac{v_\parallel}{c}\frac{e}{T_e}A_\parallel + \frac{B_\parallel}{B})F_e. \tag{7}$$

The energetic species is assumed to have a slowing down equilibrium distribution F_h, given by

$$F_h = \begin{cases} \frac{3N_h}{4\pi}\left[ln(1+\delta^{-3})(v^3 + v_c^3)\right]^{-1}, & \text{if } v \le v_\alpha \\ 0, & \text{otherwise;} \end{cases} \tag{8}$$

where $\delta = v_c/v_\alpha$, $v_\alpha = (2E_\alpha/M)^{1/2}$ is the velocity of the energetic particle at birth, $E_\alpha = 3.5MeV$ for alpha particles, and

$$v_c = (\frac{3\sqrt{\pi}}{2}\frac{m_e}{M}\frac{N_i}{N_e})^{\frac{1}{3}}(\frac{2T_e}{m_e})^{\frac{1}{2}},$$

is the typical velocity of the slowing down energetic particle.

The gyrokinetic equation for the energetic particles can be written as:

$$(\frac{\partial}{\partial t} + \frac{v_\parallel}{Rq}\frac{\partial}{\partial \theta} + i\omega_d)h = (-\frac{Ze}{M}\frac{\partial F_h}{\partial E}\frac{\partial}{\partial t} + i\frac{c}{B}\vec{k}_\perp \times n \cdot \vec{\nabla} F_h)\Phi_h, \tag{9}$$

with

$$\Phi_h = (\phi - \frac{v_\parallel}{c}A_\parallel)J_{0h} + \frac{v_\perp}{k_\perp c}B_\parallel J_{1h},$$

and h is the nonadiabatic part of the perturbed energetic ion distribution, f, defined by

$$f = hJ_{0h} + \frac{Ze}{M}\phi\frac{\partial F_h}{\partial E},$$

where Z and M are the atomic number and the mass of the energetic ion, respectively.

In the general electromagnetic stability problem, we have to include $\phi, A_\parallel$, and $B_\parallel$ as a complete description of the perturbed electromagnetic fields. To determine these perturbed fields, we need the quasi-neutrality condition, which is valid for the low frequency modes:

$$\int d^3v f_i + Z\int d^3v f = \int d^3v f_e, \tag{10}$$

and the perpendicular and parallel components of Ampere's law:

$$B_\parallel = \frac{4\pi e}{ck_\perp}\int d^3v v_\perp (J_{1i}f_i + ZJ_{1h}f_h) + \frac{2\pi m_e}{B}\int d^3v v_\perp^2 f_e, \tag{11}$$

$$k_\perp^2 A_\parallel = \frac{4\pi e}{c}[\int d^3v v_\parallel (f_i + Zf_h) - \int d^3v v_\parallel f_e]. \tag{12}$$

In Eqs. (2), (5), (9) and (10) to (12), h_i, h and h_e are functions of $v_\parallel$, $v_\perp$, t and the extended variable θ, while $\phi, A_\parallel$, and $B_\parallel$ are functions of the extended θ variable and t only. The use of $v_\parallel$ and $v_\perp$ as the velocity variables is valid in a slab geometry. In the tokamak geometry, strictly speaking, the particle kinetic energy, E, and magnetic moment, μ, should be used. However, as this detail does not affect our numerical technique and we do not want to mix the instability considered here with the trapped particles instabilities, we use $v_\parallel$ and $v_\perp$ for simplicity. Since derivatives of $v_\parallel$, and $v_\perp$ do not appear in Eqs. (2), (5) and (9), both $v_\parallel$, and $v_\perp$ are regarded as parameters in the problem. These equations form a complete set of equations that describe the low frequency electromagnetic stability of tokamak plasmas. The strategy is to use Eqs.(2), (5) and (9) to advance h_i, h and h_e to a new time step using values of $\phi, A_\parallel$, and $B_\parallel$ at the old time step. When the values of h_i, h and h_e at the new time step are known, the values of $\phi, A_\parallel$, and $B_\parallel$ can be updated using Eqs. (10) to (12). These procedures are trivial extention of previous work[7] to include the energetic species.

III. BALLOONING MODES

To investigate the ballooning modes, we impose the boundary condition on the perturbed fields such that ϕ and $B_{\parallel}$ are odd with respect to the poloidal variable θ, and $A_{\parallel}$ is even. As a first step, we compare the results of our numerical model for the background plasma (excluding the energetic species) with well known ideal MHD ballooning mode results. Figure 1 shows a plot of the energies (defined as the integral of the absolute value squared over the extended poloidal variable) of the perturbed fields of a ballooning mode as functions of time after being initialized from noise level to a linear growth stage. The parameters involved are $s = 1.0, q = 2, T_e = T_i, \eta_i = 0.5, \eta_e = 1.0, \beta_i = 0.019, k_\theta \rho_i = 0.5$, and $L_n/R = 0.2$. For this set of parameters, the background plasma pressure gradients are sufficient to destabilize the ballooning mode in a shifted circular flux surfaces tokamak equilibrium. The eigenfunctions for the perturbed fields in the linear growth stage is shown in Fig. 2. The boundary conditions are clearly satisfied for each perturbed field.

If the background ion beta values are varied, the well known results from ideal MHD of the first and second ballooning stabilities are recovered. This is shown in Figure 3, where the growth rates for the ballooning modes are plotted as functions of β_i. The two curves shown in Fig. 3 correspond to $k_\theta \rho_i = 0.25$ and 0.50. All other parameters used are the same as those in Figs. 1 and 2, unless stated otherwise. The ballooning modes are stable for β_i values outside an unstable region that separates the first and second stability regimes. These threshold values in beta shown in Fig. 3 also agree with previous results that show finite gyro-radius effects to be stabilizing because they shrink the unstable region[11].

An interesting fact we want to point out is that our approach shows that the ballooning modes in the stable regions are truely stable, i.e ., the growth rates are negative, unlike the previous work of Spong et al.[5]. In that work, the inclusion of the approximated ion magnetic drift resonance term by expansion leads to a persistent instability regardless of beta values. The 'stability boundaries' in Ref. 5 are defined as the contours of very low growth-rate value and these contours have qualitatively the same appearance as the ideal MHD ballooning stability boundaries. It is comforting that in the present approach, the MHD ballooning results are recovered (in the sense that there is a true threshold separating the stable from the unstable region) with an accurate treatment of the ion magnetic drift term.

In Fig. 4, we plot the stability regime in the shear and ion beta space. This is similar to the more commonly seen $s - \alpha$ (α is the normalized pressure gradient parameter) plot because in our case β_i differs from α by just a constant factor. Our result is qualitatively the same as the ideal MHD result. Again, the two curves corresponding to $k_\theta \rho_i = 0.50$ and $k_\theta \rho_i = 0.15$ in Fig. 4 confirm that finite gyro-radius effects are stabiiizing.

IV. ENERGETIC PARTICLE EFFECTS

Having recovered the MHD ballooning mode results for the background plasma, we proceed to investigate the effects of energetic particles on the ballooning modes by including the energetic species in our numerical model. To better unveil the effect of the energetic particles, we compare the growth rate obtained from numerical calculation with and without the energetic species and plot it with respect to the pressure gradient parameter α. In Fig. 5 the asterisks are a replot of the growth-rate data shown in Fig. 4 for $k_\theta \rho_i = 0.15$ at $s = 1.0$. On this curve, we pick a ballooning stable operating point that corresponds to $\beta_i = 0.004$ and freeze the background ion at that condition while we gradually increase the density of the energetic species, which has a slowing-down equilibrium distribution with $E_\alpha/T_i = 350.0$ (corresponding to an alpha particle population in a background ion temperature of 10 KeV). As the density of the energetic species increases, the total pressure and the pressure gradient parameter α increase. Since the background ion beta and temperature are kept fixed in this series of calculations, the electron density must increase at the same time in order to satisfy the neutrality condition. The open squares shown in Fig. 5 represent the growth-rates of the ballooning modes as the relative density of the energetic species (as indicated by the side of the open squares) increases. From Fig. 5, it is evident that as the energetic concentration increases, the growth-rate qualitatively retraces the same curve as if the background ion beta were increasing. The originally ballooning stable background plasma is first destabilized by the presence of the energetic species. The growth-rate peaks at around $N_h/N_e = 0.04$ and thereafter the growth-rate decreases with further increase in N_h/N_e. The system becomes ballooning stable again when N_h/N_e is about 0.12 to 0.14. In other words, the effects of energetic particles on ballooning modes are qualitatively similar to those of the background plasma, namely they destablize above a lower threshold and stabilize above a higher threshold. These thresholds are best characterized by the pressure gradient parameter α defined earlier.

To confirm this observation, we repeated the same series of calculations with the same set of parameters, except with a weaker shear, $s = 0.5$. We start the calculation at $\beta_i = 0.004$ where the background plasma is ballooning unstable because of the weaker shear. The results are presented in Fig. 6 in a similar manner. As the energetic density increases, the ballooning mode becomes more unstable and the growth-rate peaks when N_h/N_e is roughly 0.02. Further increases of N_h/N_e lead to smaller growth-rates and the system becomes ballooning stable when N_h/N_e is greater than 0.12. However, before the ballooning mode is stabilized, there is a spiky peak near $N_h/N_e = 0.10$, which may be due to energetic particle magnetic drift resonance. We have checked the validity of this spiky peak by refining the spatial as well as velocity space grids in the numerical code. It does not appear that this peak is not due to numerical odd effects.

V. CONCLUSIONS AND DISCUSSIONS

We have studied the stability of ballooning modes in a shifted circular flux surface tokamak equilibrium by a newly developed gyrokinetic equation solver. The energetic particles are modeled with a equilibrium slow-down distribution in energy. The gyrokinetic equations for the background ion and electron, as well as that of the energetic population, are solved directly without approximation as an initial value problem.

With the background ions and electrons only, our numerical model recovered well known results of MHD ballooning modes, in particular, the existence of a high beta second stability regime. The ballooning modes in the stable regions are truely stable and their growth rates are negative, unlike the previous work of Spong et al.[5]. In that work, the inclusion of the approximated ion magnetic drift resonance term by expansion leads to a persistent instability regardless of beta values.

When the energetic species were included, we found that their effects on ballooning stability was roughly about the same as the background plasma, in the sense that increasing energetic particle density first destabilizes the ballooning mode but then stabilizes it when the second stability threshold is exceeded. In a more detail description, energetic particles contribute to spiky secondary peaks in growth-rate, which superimpose on an otherwise smoothly varied background. These sudden jumps in growth-rate may be related to energetic particle drift resonances. However, the overall ballooning stability behavior of the system is not qualitatively changed. An important result of this work is that when the energetic particle drift resonance is treated accurately the ballooning mode is more stable than the prediction of previous approximated models[5,6].

The result presented here is encouraging because it points to the possibe improvement of confinement in a fusion reactor due to stabilization of the ballooning modes by the presence of energetic particles. Current concern over other deleterious effects of energetic particles to the confinement in a reactor regime, such as the excitation of toroidicity-induced Alfen eigenmode (TAE), may be investigated using the same approach with a slight modification of our model to include the radial mode structure. We speculate that if the energetic particle drift resonance can be treated with the same level of accuracy as in this work, the TAE mode may be more stable than current theory predicted.

5. REFERENCES

1. K. T. Tsang and D. J. Sigmar, *Nucl. Fusion* **21**, 1227 (1981).
2. J. W. Conner, R. J. Hastie, T. J. Martin, and M. F. Turner, *Proceedings of the 3rd Joint Varenna-Grenoble International Symposium* (1982).
3. M. N. Rosenbluth, S. T. Tsai, J. W. VanDam, and M. G. Engquist, *Phys. Rev. Lett.* **51**, 1967 (1983).
4. R. A. Dandl et al., *Plasma Physics and Controlled Nuclear Fusion Research* (International Atomic Energy Agency, Vienna, 1975), Vol. 2, p.141.
5. D. A. Spong, D. J. Sigmar, W. A. Cooper, D. E. Hastings, and K, T. Tsang, *Phys. Fluids* **28**, 2494 (1985).
6. G. Rewolt, *Phys. Fluids* **31**, 3727 (1988).
7. K. T. Tsang and C. Z. Cheng, *Phys. Fluids B* **3**, 688 (1991).
8. J. W. Connor, R. J. Hastie, and J. B. Taylor, *Proc. R. Soc. (London) Ser. A* **365**, 1 (1979).
9. W. M. Tang, J. W. Conner, and R. J. Hastie, *Nucl. Fusion* **20**, 1439 (1980).
10. B. Coppi, A. Ferreira, J. W.-K. Mark, and J. J. Ramos, *Nucl. Fusion* **19**, 715 (1979).
11. W. M. Tang, J. W. Conner, and R. B. White, *Nucl. Fusion* **21**, 891 (1981).

Figure Captions

Figure 1: Plot of the energies (defined as the integral of the absolute value squared over the extended poloidal variable) of the perturbed fields ϕ (solid line) , $B_{\parallel}$ (long-dashed) and $A_{\parallel}$ (short-dashed) of a ballooning mode as functions of time after being initialized from noise level to a linear growth stage. The parameters involved are $s = 1.0, q = 2, T_e = T_i, \eta_i = 0.5, \eta_e = 1.0, \beta_i = 0.019, k_\theta \rho_i = 0.5$, and $L_n/R = 0.2$.

Figure 2: The corresponding eigenfunctions for the perturbed fields of Fig. 1 in the linear growth stage. The solid lines are the real parts and the dashed lines are the imaginary parts of the eigenfunctions.

Figure 3: The growth rates for the ballooning modes plotted as functions of β_i. The two curves shown are for $k_\theta \rho_i = 0.25$ (solid line) and 0.50 (dashed line). All other parameters used are the same as those in Figs. 1 and 2.

Figure 4:The stability regions in the shear (s) and ion beta (β_i) space. The two curves are for $k_\theta \rho_i = 0.50$ (solid lines) and $k_\theta \rho_i = 0.15$ (dashed lines).

Figure 5: Growth-rate of ballooning mode versus α (total pressure gradient parameter) for an increasing concentration energetic species. The background ion beta is fixed at 0.004 and $s = 1.0$. The crosses are a replot of the growth-rate data shown in Fig. 4 for $k_\theta \rho_i = 0.15$. The open-squares are data with the energetic species.

Figure 6: Growth-rate of ballooning mode versus α (total pressure gradient parameter) for an increasing concentration energetic species. The background ion beta is fixed at 0.004 and $s = 0.5$. The crosses are a replot of the growth-rate data shown in Fig. 4 for $k_\theta \rho_i = 0.15$. The open-squares are data with the energetic species.

Fig.1

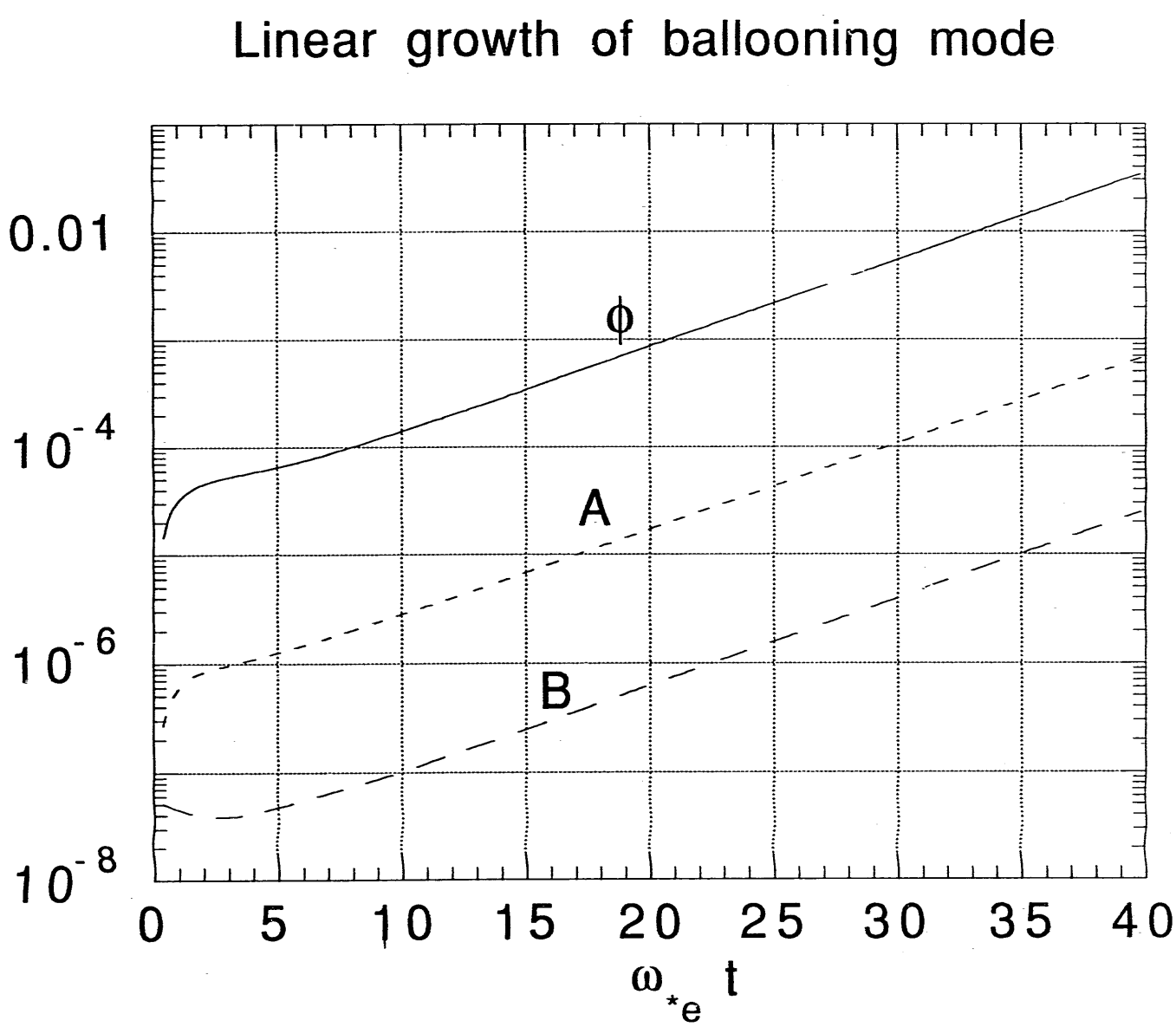
Linear growth of ballooning mode
0.01
10^-4
10^-6
10^-8
φ
A
B
0
5
10
15
20
25
30
35
40
ω*e t

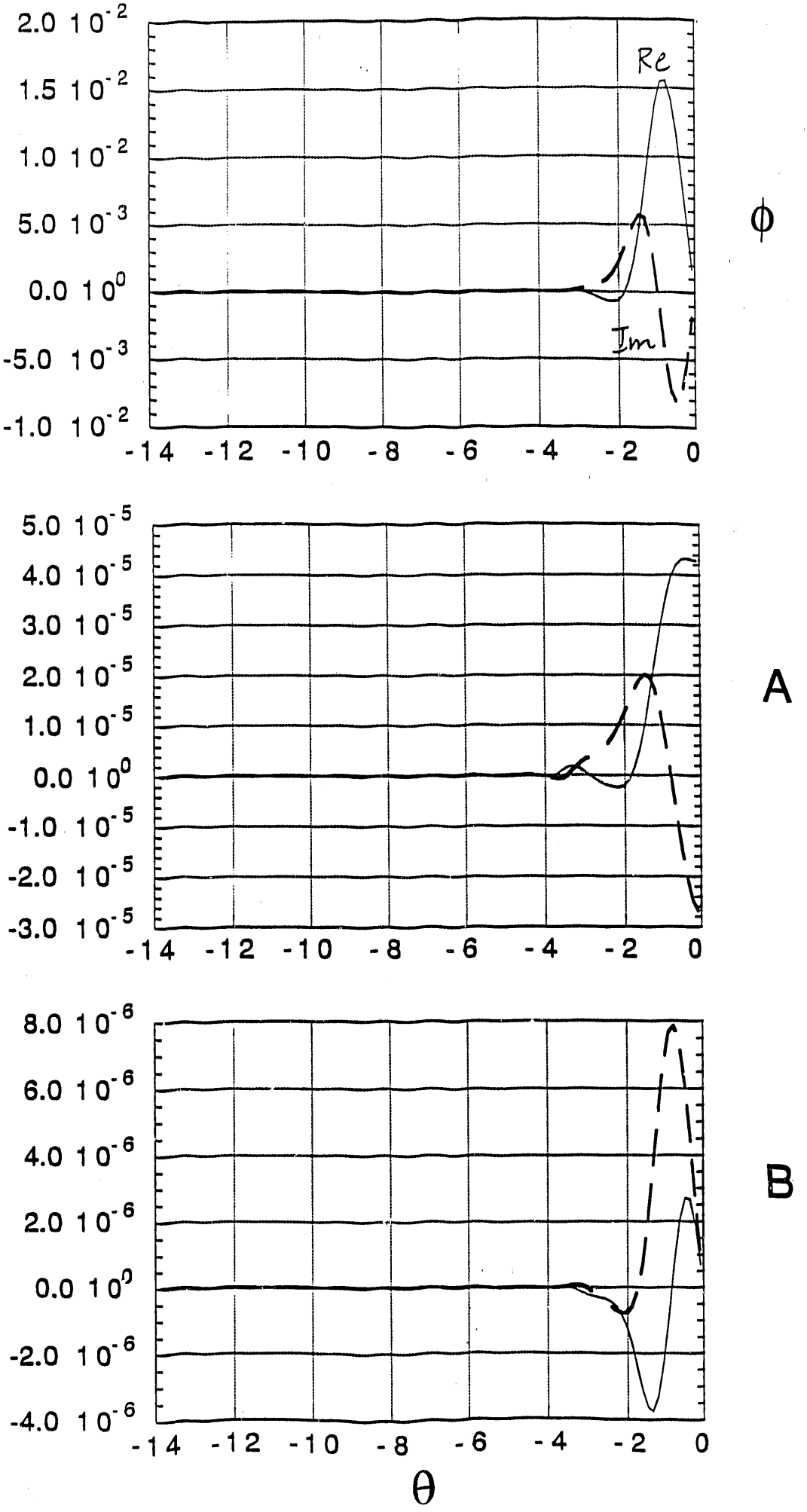
2.0 10-2
1.5 10-2
1.0 10-2
5.0 10-3
0.0 100
-5.0 10-3
-1.0 10-2
Re
Im
-14 -12 -10 -8 -6 -4 -2 0
ϕ
5.0 10-5
4.0 10-5
3.0 10-5
2.0 10-5
1.0 10-5
0.0 100
-1.0 10-5
-2.0 10-5
-3.0 10-5
-14 -12 -10 -8 -6 -4 -2 0
A
8.0 10-6
6.0 10-6
4.0 10-6
2.0 10-6
0.0 100
-2.0 10-6
-4.0 10-6
-14 -12 -10 -8 -6 -4 -2 0
B
θ

Fig.2

Fig.3

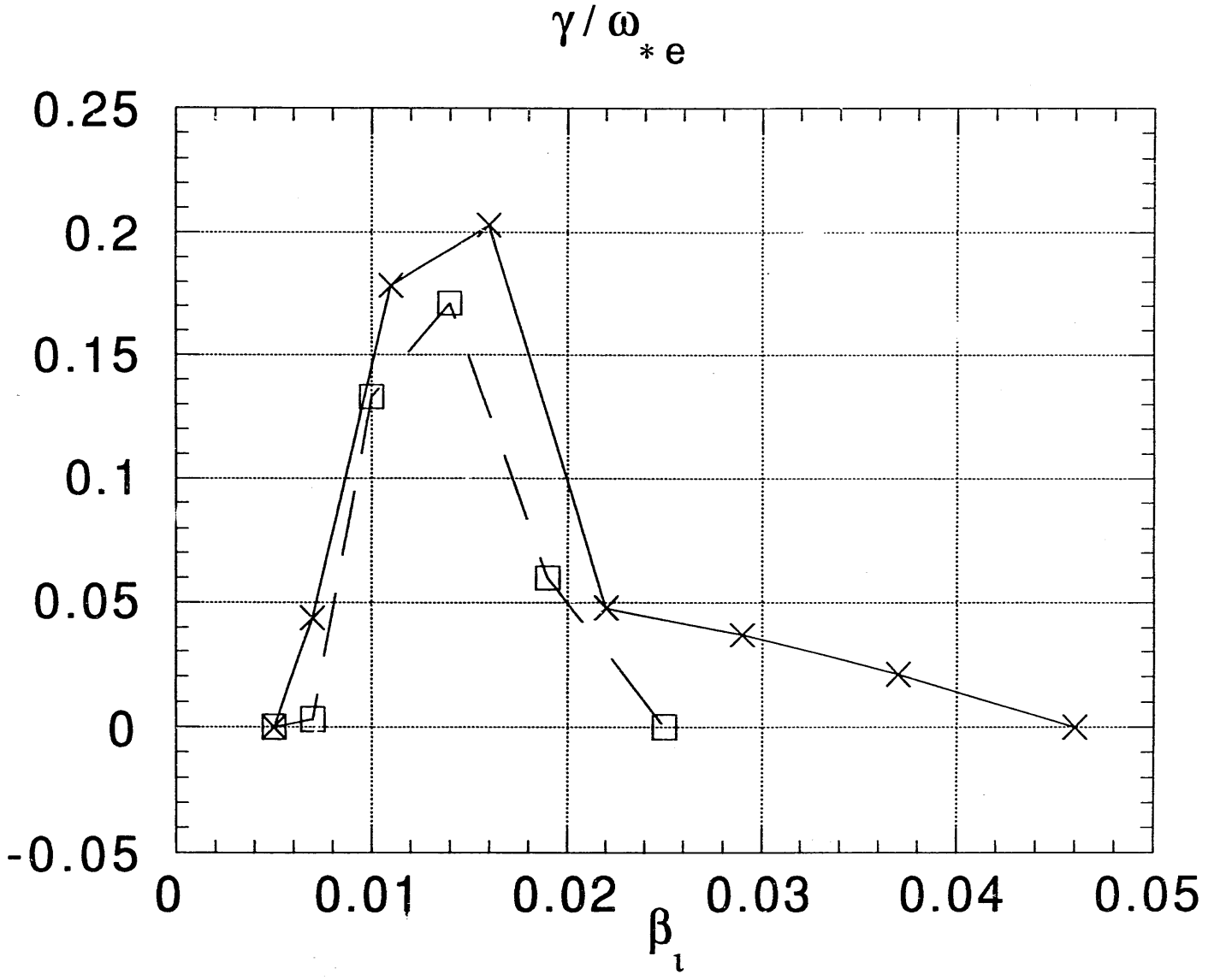

Fig.4

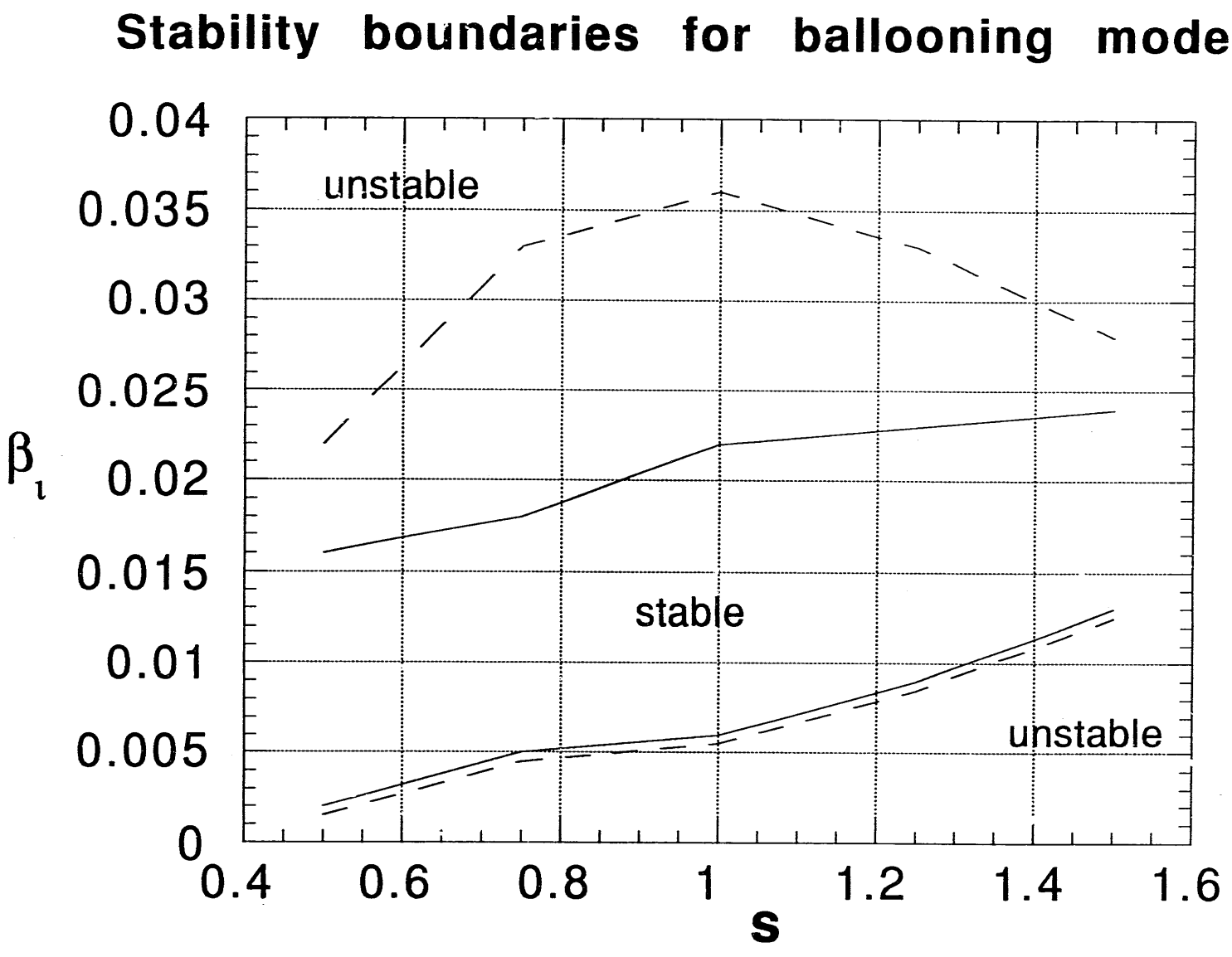
Stability boundaries for ballooning modes
0.04
0.035
0.03
0.025
0.02
0.015
0.01
0.005
0
β_i
unstable
stable
unstable
0.4
0.6
0.8
1
1.2
1.4
1.6
s

Fig.5

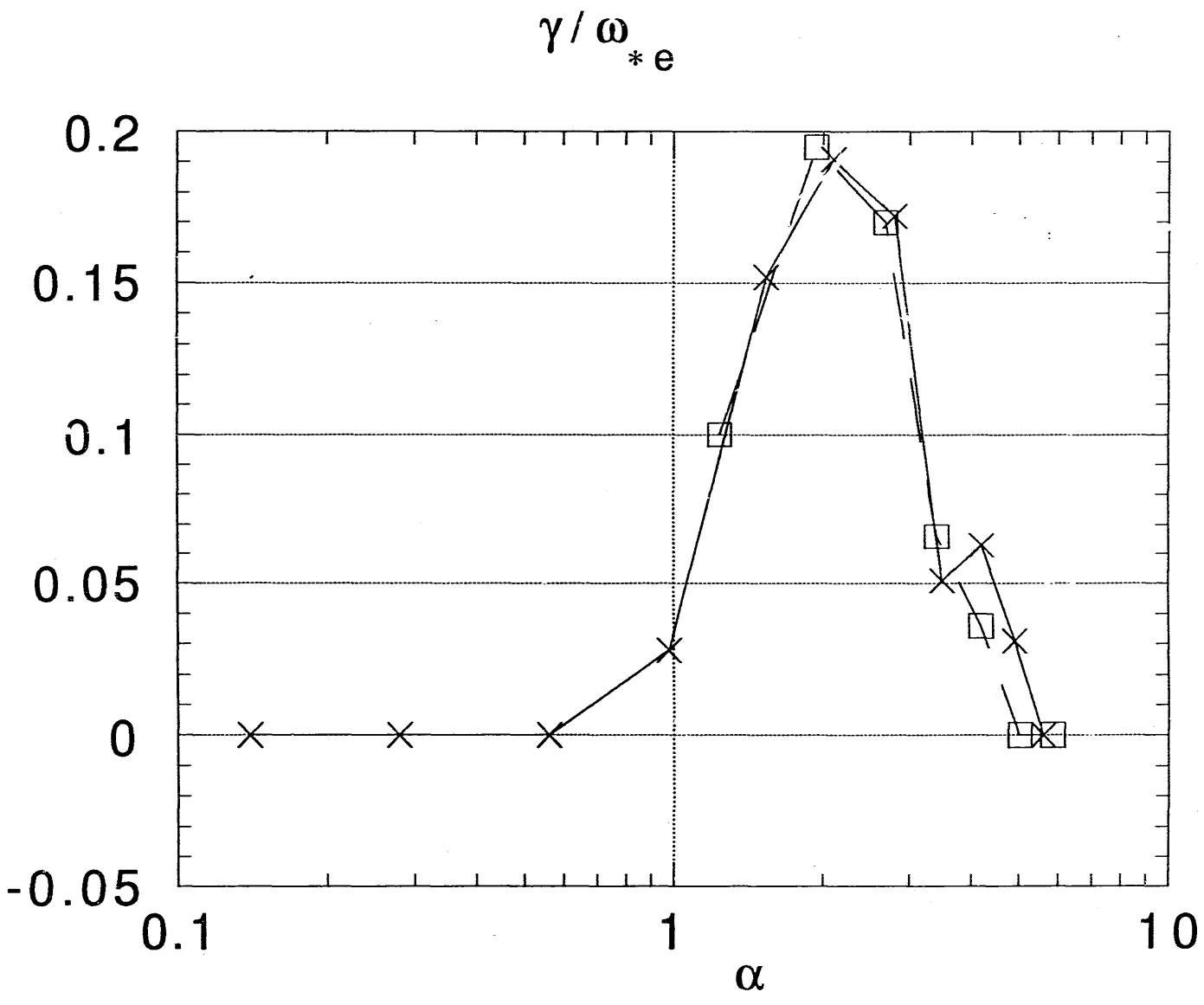

Fig.6

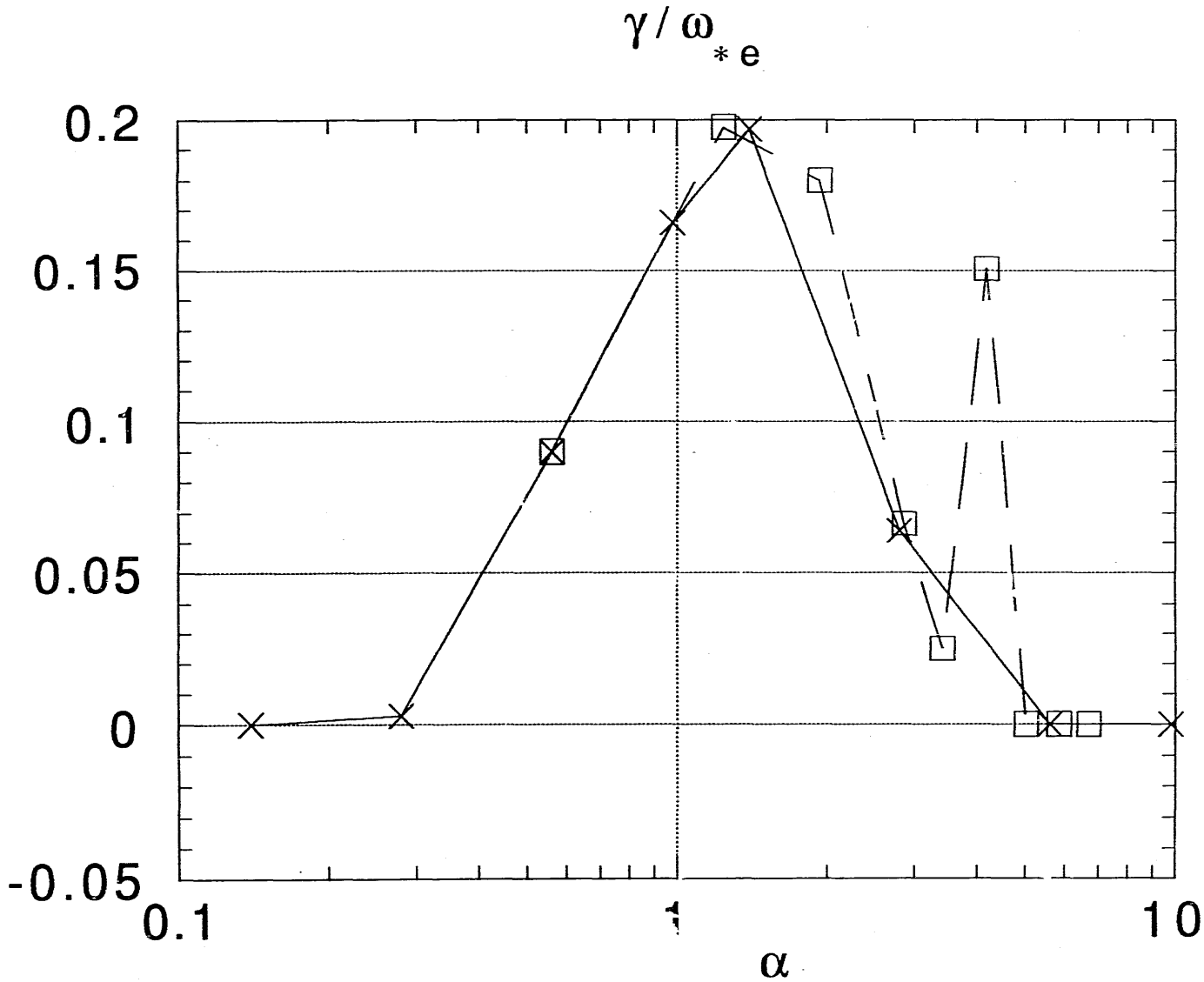

END

DATE
FILMED
3 1 4 9 2

I